SCIENCE CHINA
Technological Sciences

December 2010 Vol.53 No.12: 3356–3364
doi: 10.1007/s11431-010-4163-5

Optimization of the head shape of the CRH3 high speed train

SUN ZhenXu[1], SONG JingJing[1] & AN YiRan[1*]

College of Engineering, State Key Laboratory for Turbulence and Complex Systems, Peking University, Beijing 100871, China

Received July 15, 2010; accepted September 16, 2010

Aiming at optimizing the head shape of the CRH3 high speed train, an efficient optimization approach is proposed. The CFD analysis by solving Navier-Stokes equations is coupled with optimization calculation based on the multi-objective genetic algorithm, meanwhile the arbitrary shape deformation technique (ASD) is also introduced into the design flow, which greatly shortens the time consumption for geometry regeneration and flow field remeshing. As a result, the efficiency of the optimization calculation is highly improved. Statistical analysis is done to the designs in the design space, and the correlation between the design variables and the objective is studied to find out the key variables that most affect the objective. Response surface analysis is also performed to get the nonlinear relationship between the key design variables and the objective with the Kriging algorithm. Finally, after the optimization, an aerodynamic performance comparison between the optimal shape and the original shape reveals that the original shape of CRH3 high speed train owns a very stable aerodynamic performance and can be trustingly used in industry.

aerodynamic shape design, optimization, arbitrary shape deformation, response surface analysis, Kriging algorithm

Citation: Sun Z X, Song J J, An Y R. Optimization of the head shape of the CRH3 high speed train. Sci China Tech Sci, 2010, 53: 3356–3364, doi: 10.1007/s11431-010-4163-5

1 Introduction

High speed railway plays a vital role in economic development and social progress, especially in today's China. Massive scientific researches in the high speed railway field have been conducted in those developed countries such as Japan and France, and plentiful experience has been accumulated to develop new high speed trains with even faster speed. Safety, amenity, low energy cost and the influence on the surroundings due to the running of a high speed train are closely associated with its aerodynamic performance, which is directly dominated by its streamline design [1–3]. With a better streamliner utilized, a lower drag coefficient of the high speed train could be obtained. In brief, in order to design a new high speed train with better performance, the drag of the high speed train should be reduced as much as possible. The aerodynamic shape optimization of a new high speed train should be performed under this principle.

Practical engineering design often involves multiple disciplines. The design goal is frequently defined by multiple and sometimes conflicting design objectives, along with the huge number of design variables [4]. Besides, an optimization usually should be conducted under certain constraints, for example, the volume should be less than X and the weight should not be greater than Y. To solve such a problem, a 'systematic engineering' point of view has to be considered, which means that this kind of optimization problems have to be divided into several smaller ones, then these smaller problems are combined together under certain disciplines so as to take every design variable into consideration.

Nowadays, two kinds of approaches are utilized to optimize the shape of high speed trains all over the world: experiments and numerical simulations. Wind tunnels are

*Corresponding author (email: anyr@pku.edu.cn)

mostly used for experiments, while others such as water tunnels experiments, electricity similarity experiments and real vehicle tests are also frequently performed. Compared to numerical simulations, experiments are more popular in high speed trains' shape design. But with the rapid development of computing technology, large scale numerical simulations now become possible, which have advantages such as short investigation period, low cost, and most of all, the ability to simulate extreme conditions which cannot be met frequently in everyday life. The general process to conduct a numerical simulation is introduced here. First of all, validation for the effectiveness of the computing codes with specific experimental cases should be conducted. Secondly, massive cases are numerically simulated to find some discipline. In the end, the optimal solution is selected from the massive cases and wind tunnel experiments are performed to verify its aerodynamic performance.

The numerical approach mentioned above, in a sense, belongs to a kind of optimal selections and is greatly dependant on engineering experience. Even though a large amount of cases have been studied and some disciplines have been found, they are usually limited to a linear relationship between single design variable and the objective, and the nonlinear relations between multiple variables and the objective can never be attained. In order to overcome the disadvantages of this approach and achieve a true shape optimization, the direct optimization method has to be adopted.

From a mathematical point of view, the direct optimization method means that maximizing or minimizing the objective (for example, maximizing the lift to drag ratio of an airfoil, minimizing the drag of a locomotive) by mathematic algorithms within several possible constraints such that an aerodynamic shape design problem can be converted to a constrained optimization problem. Two kinds of algorithms are usually adopted in the direct optimization approach, namely the local algorithms and the global algorithms. As the representative of the local algorithms, gradient methods can perform optimization in the direction of the gradient of the objective function [5, 6], but unfortunately they would always suffer from getting stuck in a local optimal solution. As for the global algorithms, they could succeed in obtaining the global optimal solution and be free from the objective's sensitivity limitation to the design variables. However, deficiency still exists. This kind of algorithms belong to random search methods, with which geometry regeneration, flow field remeshing and recalculation have to be conducted for every design, leading to a relatively low computational efficiency [7].

Due to the limitation of computer hardware, flow field optimization for modern engineering design is very difficult to be applied into practice. As a three-dimensional shape-deforming flow field optimization problem, optimization of the head shape of a high speed train often leads to a low efficiency with the global algorithms utilized. In this paper, a new optimization strategy is proposed by the combination of several commercial codes. This approach possesses a relatively high efficiency due to the use of ASD technique, which could avoid the geometry regeneration and flow field remeshing procedures that always arise in ordinary shape optimization problems. Meanwhile, with the help of the global searching algorithm, this approach could be used to find the global optimal solution.

2 Optimization strategy

Three major challenges exist in three-dimensional shape optimization in the flow field: (1) the efficiency to solve NS equations repeatedly; (2) the capability to accurately describe an arbitrary three-dimensional geometric model mathematically; (3) the capability to keep or obtain a new computational grid after the shape deformation. Concerning the first challenge, in order to improve the computational efficiency, reasonable initial values should be provided before solving NS equations in order to reduce iterations and fasten the convergence. As for the second challenge, general methods are utilized to parameterize the original geometry [8]. Two different approaches can be used to face the third challenge. The first approach is to remesh the flow field after the shape deformation, which seems impractical for most engineering problems. The other one is that deformation is performed directly on the original grid and the mesh quality is maintained during the deformation process [9]. Traditional optimization usually utilizes the first approach, which costs much time in geometry deformation and flow field remeshing, resulting in a low optimization efficiency. The second approach is adopted in this paper with the use of the arbitrary shape deformation (ASD) technique. The ASD technique builds a new control volume on the basis of the original geometric model, and performs smooth, accurate, volumetric deformation directly on the grid through the movements of control points, which can greatly improve the optimization efficiency.

In the present paper two kinds of optimization commercial codes, namely SCULPTOR and modeFRONTIER, are utilized, coupled with the CFD analysis codes FLUENT to perform the optimization of the head shape of the CRH3 high speed train. Although SCULPTOR gets the ASD technique embedded, its optimization algorithms are mostly those based on gradient (such as, Newton method, sequential quadratic program method, etc.), which always lead to a local optimal solution and limit its wide use in optimization. Commercial software modeFRONTIER is a mature integrated platform for nonlinear multi-objective optimization, and has a completed system for optimization. With many kinds of high resolution optimization algorithms included, from the algorithms for design of experiment to the algorithms for optimization, a global optimal solution can be precisely captured in the design space. In this paper, mod-

modeFRONTIER is used as the platform for algorithms calling and statistical post-processing for designs in the design space. Based on this platform, SCULPTOR is coupled for mesh deformation with the use of the ASD technique and FLUENT is coupled together for CFD analysis. In order to improve the optimization efficiency and save the time for flow field calculation, an initial aerodynamic calculation for the original head shape is conducted and the converged solution is obtained. Every design in the subsequent optimization takes the converged solution as the initial value, thus the iterations to achieve convergence can be significantly reduced.

Optimization of the head shape of the CRH3 high speed train is performed in present paper, and the drag force exerted on the train is chosen to be the optimization objective. According to the knowledge of head design for a high speed train, several design variables are chosen as optimization variables, which are the nose height (NoseHeight), nose length (NoseForward), nose thickness (NoseThickness) and the height of the driving cab's roof (NoseTopChannel). These four variables can roughly depict the streamline head of the high speed train, and the streamline head can be corrected through the adjustment of the four variables. The original head shape corresponds to the four variables equal to zero. When the four variables are all negative, NoseForward means that the nose of the head is stretching forward, NoseThickness means that the nose of the head is getting thinner, NoseHeight means that the nose of the head is moving down to the ground, and NoseTopChannel means that the roof of the driving cab is moving upward. Similarly, a positive variable means a movement in the opposite direction. Meanwhile, from an engineering perspective, there exist some practical constraints in the optimization. For example, the slenderness ratio of the high speed train shouldn't be too big, the space in driving cab should be appropriate, the components in the engine carriage should be easy to install, and the driver's perspective should not be affected. So, these four variables have to be confined in a limited region. Figure 1 is the original head shape of the CRH3 high speed train, and Figures 2–5 are the deformed head shapes due to the change of the four variables.

In order to precisely capture the nonlinear relationship

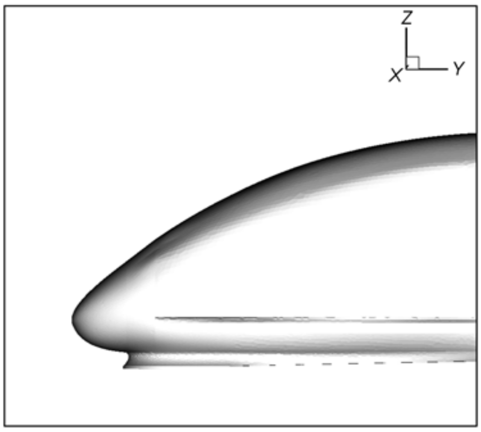

Figure 1 The original head shape.

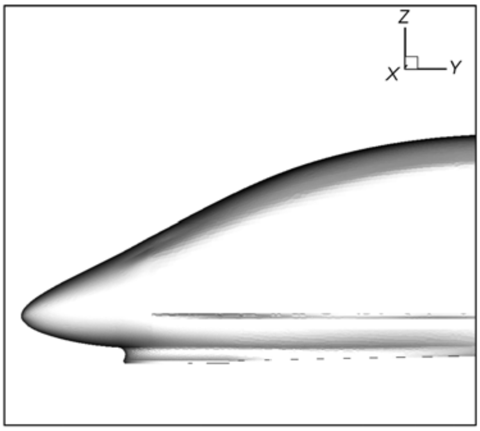

Figure 2 The deformed head shape (NoseForward).

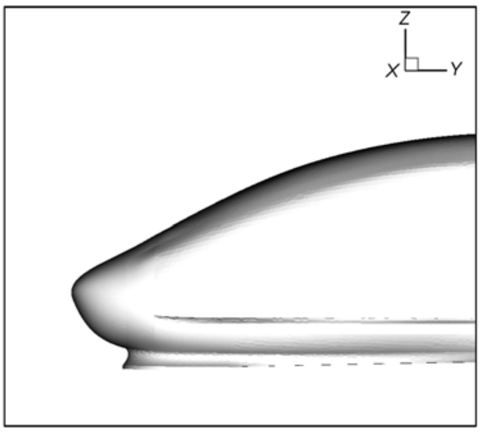

Figure 3 The deformed head shape (NoseHeight).

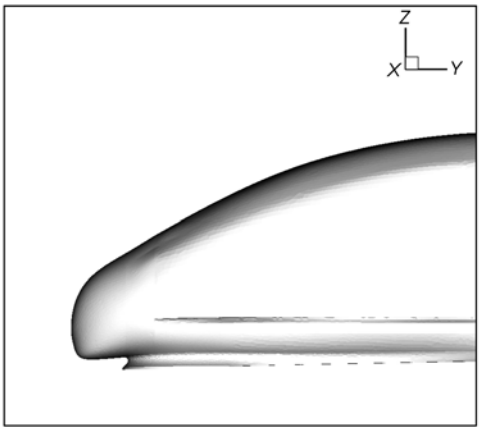

Figure 4 The deformed head shape (NoseThickness).

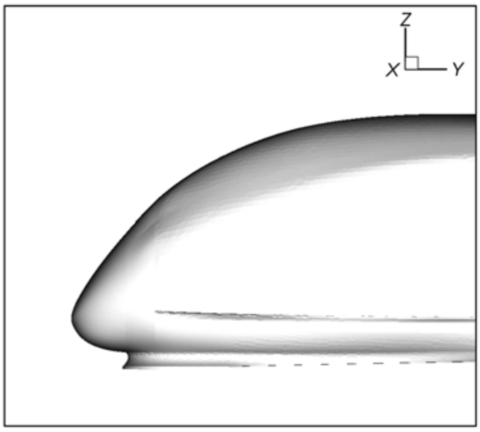

Figure 5 The deformed head shape (NoseTopChannel).

between optimization variables and the objective, designs of experiment in the design space should be elaborately initiated, based on which the optimal solution is searched for. These initial designs are very important because a better knowledge of the design space can be obtained as long as the scattering of the initial designs is more reasonable. The Sobol algorithm is utilized in this paper for the design of experiment [10, 11]. This is a kind of quasi-random algorithm which can get a more uniform scattering of initial designs compared to the random algorithm. The MOGA-II algorithm is used for optimization, which inherits the randomness and high parallelism from genetic algorithms. Response surface approximation based on the designs in the design space is performed after the optimization [12] so as to give a more accurate nonlinear relationship in the design space.

The overall design flow is shown in Figure 6.

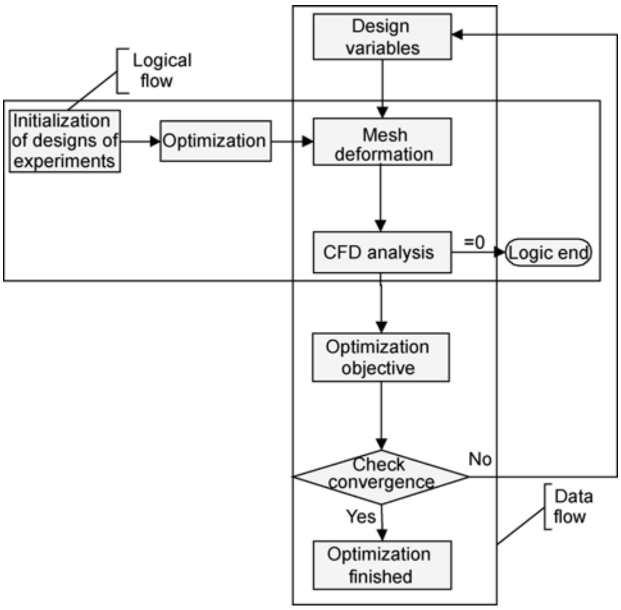

Figure 6 Overall design flow for optimization.

3 Algorithms

3.1 ASD technique

For arbitrary shape deformation technique, an ASD volume is initially built around the grid zone to be optimized. A basic ASD volume contains control points and the connections between them. Grid deformation is achieved by the movements of control points, in which C^1 continuity could be maintained. This insures the grid to be smoothly deformed, even in some large deformation conditions. Meanwhile, in order to keep the invariance of *y*+ around the computational geometry, additional layer of ASD control volume should be built along the prism mesh. When the grid deformation is performed, the control points on the additional layer mentioned above and the control points around the computational geometry should be moved synchronously, such that the prism mesh around the computational geometry could be kept invariant. This technique provides a possibility for the optimization of complicated geometry.

3.2 MOGA-II algorithm

Traditional multi-objective genetic algorithms introduce the concept of Pareto optimal frontier [13], and the correlated idea of dominance: By definition, Pareto solutions are considered optimal because there are no other designs that are superior in all objectives. A typical procedure for genetic algorithms is as follows:

(1) Randomly generate the population.

(2) Calculate each individual's value of the objective function and constraint functions.

(3) Classify the population on the basis of objective function's value.

(4) Calculate each individual's constraint penalty function, Pareto penalty function and total penalty function on the basis of constraint function and classification.

(5) Calculate each individual's fitness according to its total penalty function.

(6) Do operation such as selection, crossover and mutation for the born of new generation.

(7) Individuals whose total penalty equal zero are put into a candidate list. Those near to the Pareto set are retained and the others are discarded.

(8) Convergence is checked. Go to step 2 if not converged.

(9) Individuals who are too close to other individuals are eliminated.

(10) Output the Pareto set and the corresponding objective values from the candidate list.

Compared to traditional multi-objective genetic algorithms, MOGA-II improves its efficiency by a smart multi-search elitism, which can preserve some excellent solutions without bringing a premature convergence into local optimal fronts. Meanwhile, it is worth mentioning that even though this algorithm is designed for solving multiple objectives, it is still effective for single-objective optimization. In the present paper, 6 generations are used for the optimization. The ratio of crossover is 50%, the ratio of selection is 5%, and the mutation ratio is 10%.

3.3 Algorithms for CFD

The flow under consideration is a three-dimensional incompressible steady viscous flow. The primary transport variables of the flow field are the static pressure p and the velocity, which can be split into the mean velocity term $\boldsymbol{u}$ and the fluctuation term u'. These variables are governed by Reynolds averaged conservation equations of mass and momentum:

$$\frac{\partial u_i}{\partial x_i}=0, \tag{1}$$

$$\rho u_j\frac{\partial u_i}{\partial x_j}=-\frac{\partial p}{\partial x_i}+\frac{\partial}{\partial x_j}\left[\mu\left(\frac{\partial u_i}{\partial x_j}+\frac{\partial u_j}{\partial x_i}\right)\right]+\frac{\partial}{\partial x_j}(-\rho\overline{u_i'u_j'}), \tag{2}$$

where ρ and μ are the fluid density and the molecular viscosity, respectively. For the last term, $\overline{u_i'u_j'}$ is the Reynolds stress tensor term, taking the form:

$$\rho\overline{u_i'u_j'}=-\mu_t\left(\frac{\partial u_i}{\partial x_j}+\frac{\partial u_j}{\partial x_i}\right)+\frac{2}{3}\delta_{ij}\rho k, \tag{3}$$

where μ_t is the turbulent viscosity, which is expressed as $\mu_t=\rho C_\mu\frac{k^2}{\varepsilon}$. k and ε are the turbulent kinetic energy and the turbulent rate of dissipation. For a standard k-ε model [14], they are governed by the respective transport equations:

$$\rho\frac{\partial}{\partial x_i}\cdot(ku_i)=\frac{\partial}{\partial x_i}\cdot\left[\left(\mu+\frac{\mu_t}{\sigma_k}\right)\frac{\partial k}{\partial x_i}\right]-\rho\varepsilon-\rho\overline{u_i'u_j'}\frac{\partial u_i}{\partial x_j}, \tag{4}$$

$$\rho\frac{\partial}{\partial x_i}\cdot(\varepsilon u_i)=\frac{\partial}{\partial x_i}\cdot\left[\left(\mu+\frac{\mu_t}{\sigma_\varepsilon}\right)\frac{\partial \varepsilon}{\partial x_i}\right]-C_{\varepsilon 2}\rho\frac{\varepsilon^2}{k}-C_{\varepsilon 1}\frac{\varepsilon}{k}\rho\overline{u_i'u_j'}\frac{\partial u_i}{\partial x_j}. \tag{5}$$

The closure coefficients in the model are

$C_\mu=0.09,\ C_{\varepsilon1}=1.44,\ C_{\varepsilon2}=1.92,\ \sigma_k=1.0,\ \sigma_\varepsilon=1.3.$

4 Results and discussion

4.1 Computational grids and conditions

The streamline head is the objective that we mainly focus on, so that other parts that may introduce significant aerodynamic drag loads such as pantograph are all ignored. The place just before the nose of the CRH3 high speed train is a stagnation region, in which flow variables experience a sudden change in gradient. Therefore, the body is meshed very fine around the nose. As the mesh progresses backward from the nose, the mesh size is enlarged slightly to help to reduce the computational time. Fine prism grids are used so as to accurately mimic the flow behavior around the body. The total grids used in this paper are around 730 thousands, and the grids on the nose are depicted in Figure 7.

An uniform velocity flow condition is utilized with a speed of 83.33 m/s at the inlet boundary, and the ground is set to be a moving wall with the same speed as the inlet boundary. A pressure outlet condition is imposed on the outlet boundary with a 0 Pa gauge pressure. The reference pressure is set to be 1 atm. Convergence is achieved after about 9000 iterations for the original head shape. Optimization is conducted on the basis of this convergent solution.

4.2 Optimization analysis

There are 16 initial designs of experiment in the design space and 6 generations used for the optimization, so that 96 designs are obtained after the optimization. The drag history for all the designs is depicted in Figure 8.

As seen in Figure 8, the drag tends to diminish along with the optimization progress, which means the head's shape evolves into the direction of diminishing drag loads.

Statistical analysis has been performed between the design variables and the objective to reveal their correlations, as shown in Figure 9.

As seen in Figure 9, a positive correlation between the variable NoseForward and the objective within a certain range can be found, meaning that a longer nose length would lead to a lower drag force and a shorter nose length would leads to a higher drag force. The other three variables

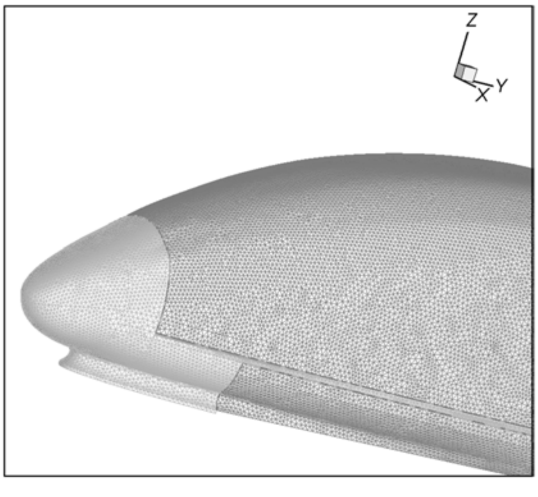

Figure 7 A side view of grids on the streamlined head of CRH3 high speed train.

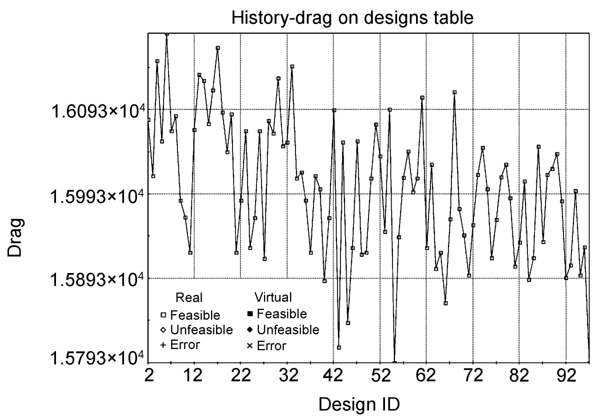

Figure 8 The drag history for all the designs.

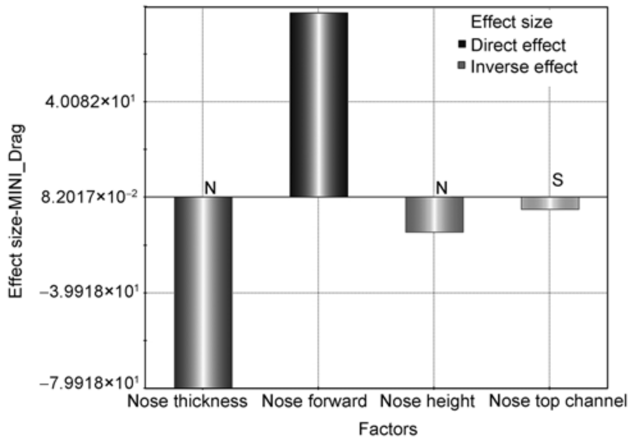

Figure 9 Correlation between the design variables and the objective.

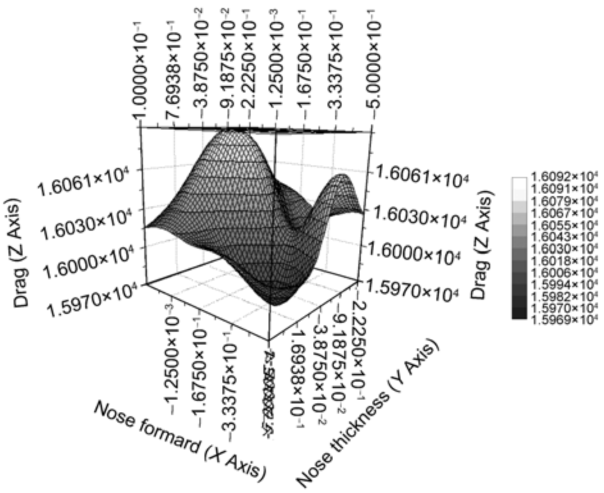

Figure 10 Three-dimensional response surface.

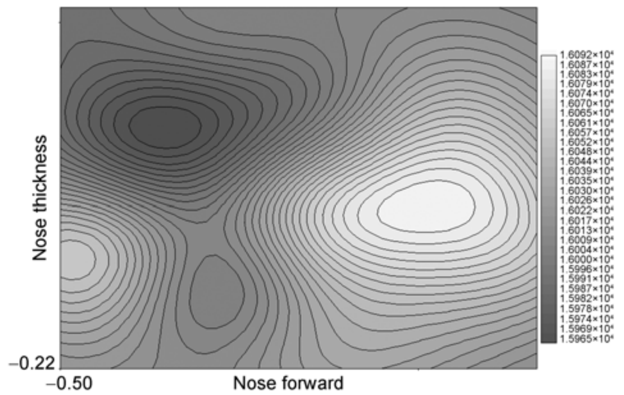

Figure 11 Two-dimensional response surface.

are negatively correlated with the objective, for example, a thinner nose would lead to a lower drag force. From the magnitude point of view, the objective is more sensitive to two design variables, namely the nose thickness and the nose length, respectively. On the contrary, the other two variables have little influence on the drag force.

In order to further dig the nonlinear relationship between the design variables and the objective, response surface analysis between the drag force and the two more sensitive variables such as NoseForward and NoseThickness is conducted. The three-dimensional surface and two-dimensional surface fitted by the Kriging method [15, 16] are shown in Figures 10 and 11.

It can be seen clearly that no pure linear relationship exists between the objective and the two variables. A higher drag force would be obtained if the nose is too much longer or too much thicker. The exact relationships in the design space are shown in Figures 12 and 13.

The nonlinear relationship can be correctly obtained, as shown in Figures 12 and 13, which can never be attained by the optimal selection method. Meanwhile, a higher drag force would be obtained based on these two variables than that based on the four variables, indicating that even though the other two variables are not so sensitive to the drag force, they still play a positive role in optimizing the head shape.

4.3 Aerodynamic analysis

After the optimization, an optimal solution is obtained with a drag force of 1.5793e4N. Compared to the original drag force which is 1.6091e4N, the optimal solution makes a reduction of 1.85% in the drag force. On the other hand, optimization of the drag force should not at the expense of deteriorating the lift force. In the present case, a lift of –5128 N is acting on the original head whist a lift of –6022 N exists on the optimal solution. A bigger downward force could be obtained by the alteration of head shape, which could enforce the stability when the high speed train is running.

The corresponding values of the design variables are –0.465 for NoseForward, 0.115 for NoseHeight, 0.245 for NoseThickness, and 0.64 for NosTopChannel. A comparison between the original head shape and the optimal one is depicted in Figures 14 and 15.

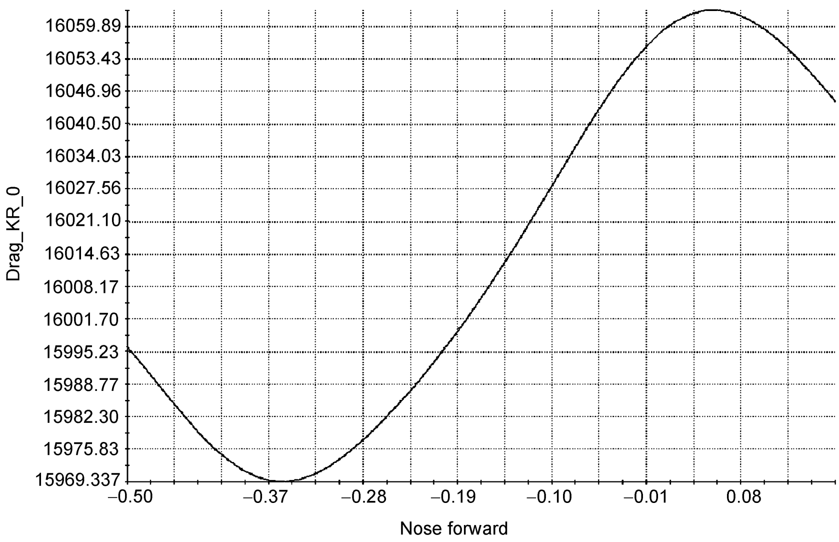

Figure 12 Relationship between the drag force and NoseForward.

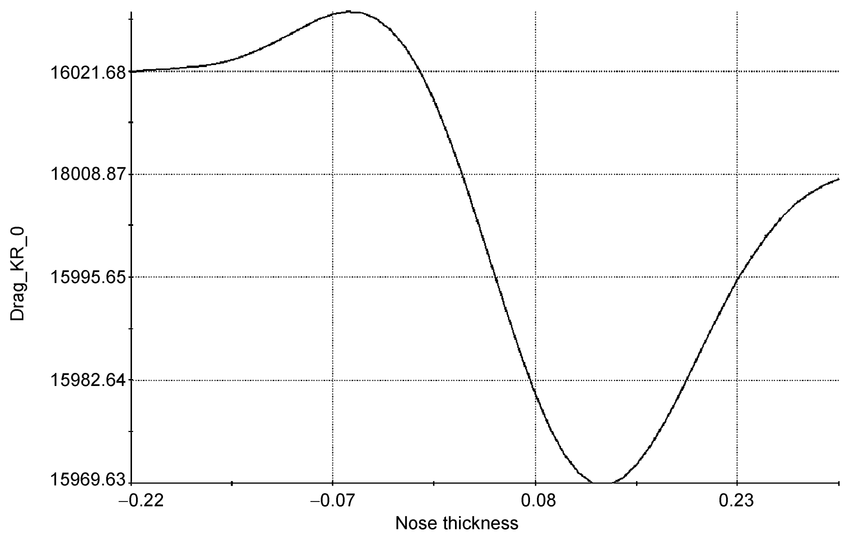

Figure 13 Relationship between the drag force and NoseThickness.

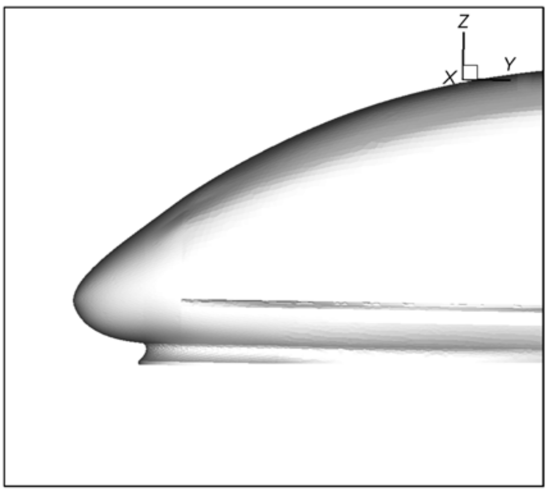

Figure 14 Original head's shape.

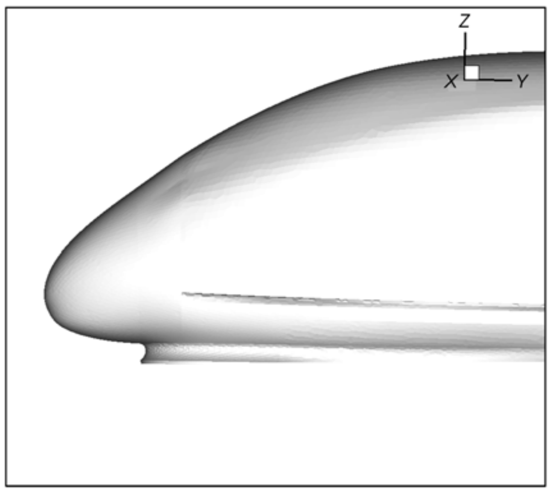

Figure 15 Optimal head's shape.

Compared to the original head shape, the optimal one makes several changes. Its nose becomes relatively longer and thicker, the nose height is slightly higher and the roof of the driving cab is a little taller.

The pressure force makes a main part of the total drag force in the aerodynamic calculation of the CRH3 high speed train. The change of the head shape would directly affect the pressure distribution on the head's surface, and further change the total drag force. Pressure distributions along the head of the original shape and the optimal one are shown in Figures 16 and 17.

The region just in front of the nose is a stagnation zone, in which the flow experiences a low velocity and very high pressure. When the flow comes across the nose tip, the velocity increases and the pressure rapidly goes lower with the increase of flow area. The high pressure zone is the main source of the drag force on the high speed train. It can be seen from the above two figures that drastic changes of maximum positive pressure (pressure above 3360 Pa) on the nose tip exist between the two shapes. For the original head shape the maximum positive pressure distributes horizontally while the maximum positive pressure distributes vertically for the optimal head shape, although they both share nearly the same area. Investigation on the pressure zone distributing from 1680 to 3360 Pa reveals that bigger operating area exists in the front of the original head while relatively smaller operating area exists only near the middle zone of the optimal head.

A comparison of pressure distributions on the symmetric plane between the two shapes is shown in Figures 18 and 19.

As Figures 18 and 19 show, a relatively bigger negative pressure zone just below the nose's tip exists in the optimal head compared to the original head, which would result in a bigger down force and a slightly smaller drag force. Besides, in the concave zone just behind the nose, a smaller positive

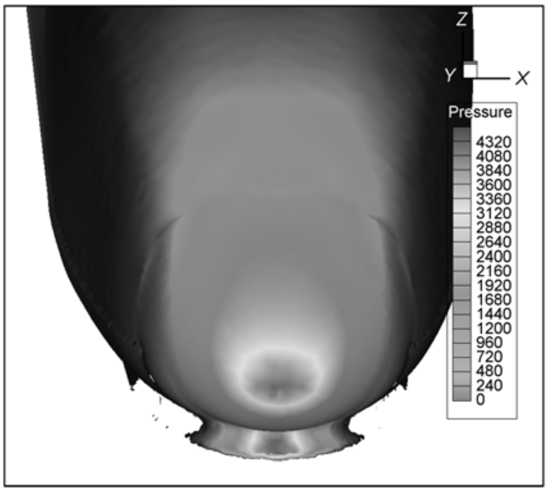

Figure 16 Pressure contour of the original shape.

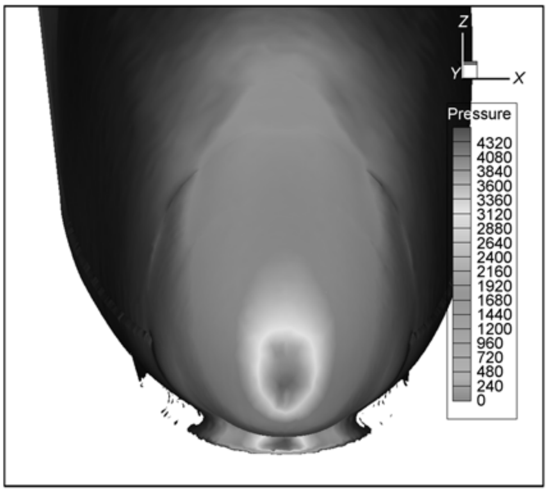

Figure 17 Pressure contour of the optimal shape.

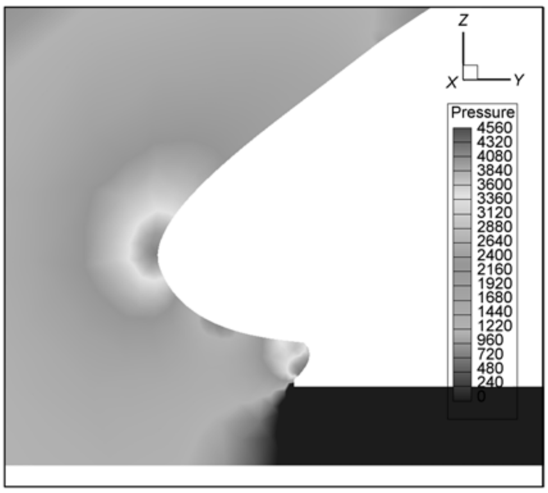

Figure 18 Pressure contour along the symmetric plane of the original head.

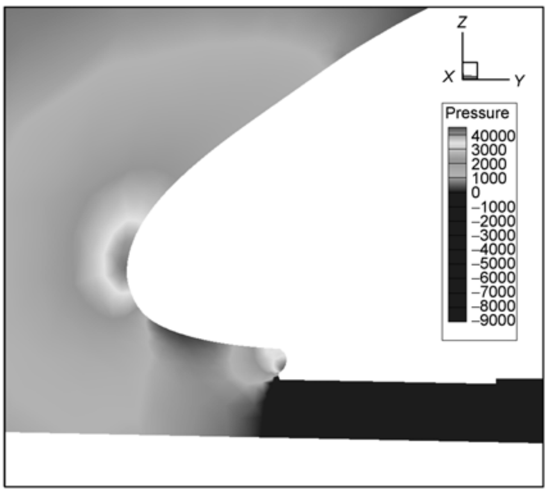

Figure 19 Pressure contour along the symmetric plane of the optimal head.

pressure region exists in the optimal head, which could lower the drag force more than the original head.

5 Conclusion

It seems more and more difficult for modern engineering design because of the complexity of design variables and the internal contradiction among them, which makes a request that modern optimization has to be conducted in a 'systematic engineering' manner so as to take every contributing factor into consideration. This discipline is followed in this paper, and the optimization of the head's shape of the CRH3 high speed train is performed with MOGA-II algorithm, which overcomes the limitations that traditional design approaches for high speed train undergoes.

With the global optimization algorithm, the global optimal solution can be guaranteed and the direct relationships between the design variables and the objective can be obtained. An obstacle that prevents the optimization method from being popularly used is the huge cost of computational time due to the shape deformation and flow field remeshing. The ASD technique is utilized in the present paper which can directly perform deformation on the mesh, so that a high efficiency has been achieved. It proves to be reliable and highly efficient through the optimization calculation of the head's shape of the CRH3 high speed train.

Our results show that the optimal solution can be obtained when the design variables take values of –0.465, 0.115, 0.245, and 0.64 for NoseForward, NoseHeight, NoseThickness and NoseTopChannel, respectively. A reduction of 1.85% in the drag force has been achieved. Correlation analysis between the design variables and the objective has been performed and the design variables most sensitive to the objective are determined. The response surface analysis between the two variables and the objective has also been carried out, and the three-dimensional response surface fitted by Kriging method obtained. Meanwhile, the nonlinear relationships between the sensitive design variables and the objective are also captured.

In addition, it can be seen that the scattering of the drag force in the design space is highly limited in a small region, which means the original head's shape of the CRH3 high speed train owns strong aerodynamic robustness.

The drag force property acts non-sensitively to the design variables within a certain range, which should be a basic property for a mature streamline head shape.

1 BAKER C. The flow around high speed trains. J Wind Eng Ind Aerod, 2010, 98(6-7): 277–298
2 Raghunathan R S, Kim H D. Aerodynamics of high-speed railway train. Prog Aerosp Sci, 2002, 38(6-7): 469–514
3 Brockie N J W, Baker C. The aerodynamic drag of high speed trains. J Wind Eng Ind Aerod, 1990, 34(3): 273–290
4 Miettinen K. Nonlinear Multi-objective Optimization. USA Norwell Massachusetts: Kluwer Academic Publishers, 1999
5 Pandya M J, Baysal O. Gradient-based aerodynamic shape optimization using alternating direction implicit method. J Aircraft, 1997, 34(3): 346–352
6 Newman J C, Taylor A C, Barnwell R W, et al. Overview of sensitivity analysis and shape optimization for complex aerodynamic configurations. J Aircraft, 1999, 36(1): 87–96
7 Deb K. Multi-objective genetic algorithms: problem difficulties and construction of test problems. Evol Comput, 1999, 7: 205–230
8 Alexa M, Behr J, Cohen R D, et al. Computing and rendering point set surfaces. T Vis Comput Gr, 2003, 9(1): 3–15
9 Kobbelt L P, Bareuther T, Seidel H P. Multi-resolution shape deformations for meshes with dynamic vertex connectivity. Comput Graph Forum, 2000, 19(3): 249–259
10 Sobol I M, Shukman B V. Random and quasi-random sequences: Numerical estimates of uniformity of distribution. Math Comput Model, 1993, 18(8): 39–45
11 Sobol I M. Uniformly distributed sequences with an additional uniform property. USSR Comput Math Math Phys, 1976, 16(5): 236–242
12 Goel T, Vaidyanathan R, Haftka R T, et al. Response surface approximation of Pareto optimal front in multi-objective optimization. Comput Meth Appl Mech Eng, 2007, 196(4-6): 879–893
13 Elaoud S, Loukil T, Teghem J. The Pareto fitness genetic algorithm: Test function study. Europ J Operat Res, 2007, 177(3): 1703–1719
14 Jones W P, Launder B E. The prediction of laminarization with a two-equation model of turbulence. Int J Heat Mass Transfer, 1972, 15(2): 301–314
15 Sakata S, Aahida F, Zako M. Hybrid approximation algorithm with Kriging and quadratic polynomial-based approach for approximate optimization. Int J Num Meth Eng, 2006, 70(6): 631–654
16 Sakata S, Aahida F, Zako M. On applying Kriging-based approximate optimization to inaccurate data. Comp Meth Appl Mech Eng, 2007, 196(13-16): 2055–2069